



# City Research Online

## City St George's, University of London

**Citation:** Kovacevic, A., Stosic, N., Jiang, Y., Furmanczyk, M. & Lowry, S. (2014). Influence of approaches in CFD Solvers on Performance Prediction in Screw Compressors. Paper presented at the 22nd International Compressor Engineering Conference, 14-17 Jul 2014, West Lafayette, USA.

This is the accepted version of the paper.

This version of the publication may differ from the final published version. To cite this item please consult the publisher's version.

**Permanent repository link:** <https://openaccess.city.ac.uk/id/eprint/15131/>

**Copyright and Reuse:** Copyright and Moral Rights remain with the author(s) and/or copyright holders. Copies of full items can be used for personal research or study, educational, or not-for-profit purposes without prior permission or charge, unless otherwise indicated, provided that the authors, title and full bibliographic details are credited, a hyperlink and/or URL is given for the original metadata page and the content is not changed in any way. For full details of reuse please refer to [City Research Online policy](#).

# Influence of approaches in CFD Solvers on Performance Prediction in Screw Compressors

Ahmed KOVACEVIC<sup>1\*</sup>, Sham RANE<sup>1</sup>, Nikola STOSIC<sup>1</sup>,  
Yu JIANG<sup>2</sup>, Michal FURMANCZYK<sup>2</sup> and Sam LOWRY<sup>2</sup>

<sup>1</sup>Centre for Positive Displacement Compressor Technology,  
City University London, EC1V0HB, UK.  
a.kovacevic@city.ac.uk

<sup>2</sup>Simerics Inc., Huntsville, AL 35801, USA.  
yj@simerics.com

\* Corresponding Author

## ABSTRACT

Computational Fluid Dynamics (CFD) offers insight into screw compressor designs beyond the capabilities of other conventional methods. It allows evaluation of local flow patterns which influence performance but are difficult or impossible to investigate experimentally. Implementation of CFD in these machines is challenging due to the physics of the flow, the properties of the working fluids and the complexity of flow passages which change size and position. This is additionally challenged by a lack of methodologies available to generate the meshes required for the full three dimensional transient simulations. Commercially available CFD solvers need to fully interact with customized grid generators to enable resolution of grid deformation during a flow solution. However, the factors that influence flow predictions are not only related to grids but also to the approach which CFD solvers use to calculate distribution of parameters such as pressure, velocities, temperatures, etc.

In this paper, two approaches most commonly used in commercial CFD software are compared and analysed. The first is a segregated cell-centre based solver and the second is a coupled vertex-centre based solver. Both are pressure based finite volume solvers. Customized grid generation software is used for meshing of moving rotors and flow domains around the rotors in an oil free air screw compressor with 'N' rotor profile of 3/5 lobe combination. The deforming rotor grid is maintained as identical in both solvers. The performance predictions obtained by calculations with these two CFD models are compared with measurements obtained on the test compressor in the City University London test rig. The comparison includes pressure in the compressor chamber, mass flow rate, indicated power and the volumetric efficiency. The study reveals differences between the results obtained by two different solvers and the experimental results. Analysis presented in this paper provides a good basis for further consideration of differencing schemes and other characteristics and settings for different CFD solvers in order to achieve accurate predictions of flows in positive displacement machines.

## 1. INTRODUCTION

Rotary Screw Compressors are positive displacement machines widely used in refrigeration, oil and gas and other industries. The working chamber of these machines consists of a pair of helical rotors that tightly mesh with each other and rotate inside a casing. Figure 1 shows a typical cycle of operation with the variation of chamber volume and pressure. The cycle starts when the screw lobes begin to form a volume that increases with rotation and enables gas admission in the interlobes. With further rotation, these pockets disconnect from the suction port. This disconnection usually occurs at the position in which the interlobe volume achieves its maximum value. Further rotation of the rotors causes a reduction of the chamber volume and an increase in the gas pressure and temperature.

When the rotors reach the discharge port, this volume connects to the discharge domain. The maximum efficiency of the cycle is reached when the internal and external pressures are matched at the position of opening the working chamber to the discharge port. Thermodynamic chamber models are commonly used in the design and analysis of twin screw compressors (Kauder and Rau, 1994, Hanjalic and Stosic, 1997). These help in the early design stages to predict performance and give general characteristics of a screw machine. Within the past decade, Computational Fluid Dynamics (CFD) has been increasingly used as a tool for design improvements in the screw compressors, particularly for compressor ports (Kovacevic et al., 2007, Voorde et al., 2005, Pascu et al., 2012).

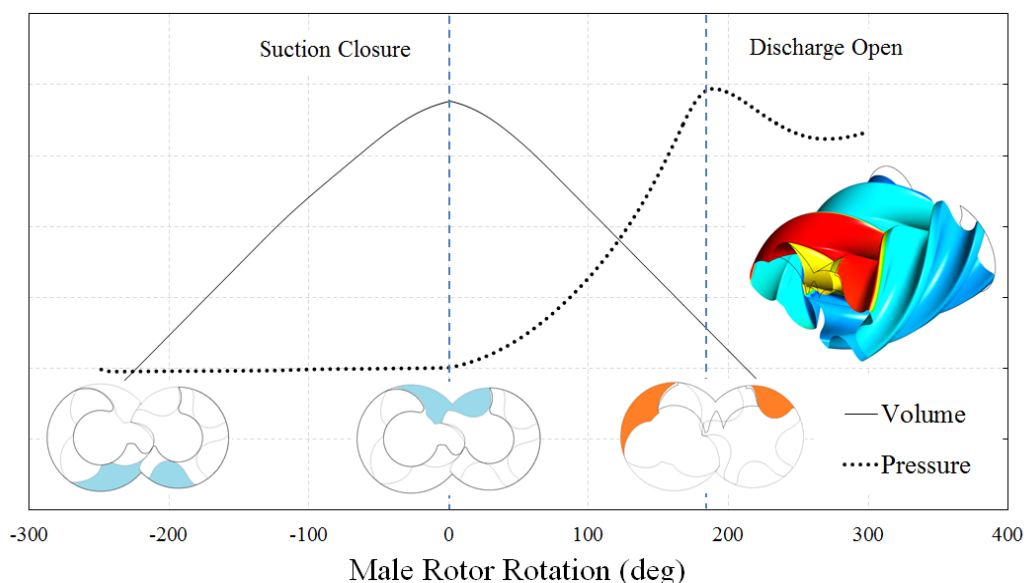


**Figure 1.** Typical Pressure and Volume variation in a Screw Compressor

The challenge in implementing CFD in positive displacement screw machines is the physics of the flow, the properties of working fluids and the complexity of the flow passages which change size and position in time. Commercially available CFD solvers need to fully interact with customized grid generators to enable resolution of grid deformation during flow solution. A breakthrough was achieved in 1999 when the rack generation method originally described by Stosic (1998) was applied to generate numerical grids for twin screw rotors by Kovacevic (1999). The first grid generator for screw compressors was based on analytical grid generation principles which allowed variety of CFD solvers to calculate performance of screw compressors, (Kovacevic et al., 2002). Since then several activities have been reported on CFD analysis of twin screw compressors. Kovacevic et al., (2007) have presented various grid generation aspects for twin screw compressors and reported results from CFD simulations of twin screw machines for prediction of flow, heat transfer and fluid-structure interaction. Results obtained with Comet and StarCD software were validated by use of Laser Doppler Velocimetry (Kovacevic et al., 2009, Kethidi et al., 2011). Pascu et al., (2012) have reported use of the same grid generation tools for design of the discharge port in an oil-free screw compressor. Sauls and Branch (2013) have utilized data from full scale CFD models to improve one dimensional leakage formulation in their thermodynamic chamber models. Hauser and Beinert (2013) compared CFD models and experimental measurements of pressure pulsations in the discharge chamber of a screw compressor to predict the effect of operating parameters on gas pulsation. Rane et al. (2013) have extended the same grid generation framework towards variable geometry twin screw rotors and reported an influence on the performance of rotor lead and profile variations.

However, the factors that influence flow predictions are not related to grids only but also to the approach which CFD solvers use to calculate the distribution of parameters such as pressure, velocities, temperatures, etc. Kovacevic and Rane (2013) have evaluated a dry twin screw expander using CFD for a range of operating conditions and compared the results with measured data provided by Dortmund University. It was found that the CFD prediction better align to measurements at higher speeds than at lower speeds. Similarly higher deviations were reported at higher pressure ratios. Some other recent studies, not published, have also reported differences between CFD predictions and measurements. It is therefore necessary to further investigate the influence of CFD model

parameters, and the different solver formulations currently available for solving flows in screw machines. The objective of this paper is to compare two commonly used solvers in commercial CFD software. The first is a coupled vertex-centre based solver which is implemented in *ANSYS CFX* (2011) and has been commonly used for screw compressor analysis. The second is the segregated cell-centre based solver used in *PumpLinx* (2014). Both are pressure based finite volume solvers. The later segregated solver has been frequently used for modelling flow and cavitation in pumps and piston and scroll compressors. Recent development in the solver allows it to be used for modelling of twin screw compressors. *Jiang et al.*, (2007) have reported the analysis of crescent oil pumps using this solver and compared predictions with the experimental results. *Wang et al.* (2012) have modelled a vane oil pump using the segregated solver and coupled it with an ODE kinetics model of the control spring. This pump performance was also compared with experimental results. Both cases provided good relationship between the model and measurements.

In this paper, the grid generation software SCORG<sup>®</sup> (*Kovacevic*, 2007) is used for meshing the moving rotor domains in the oil free air screw compressor with 'N' rotor profile of 3/5 lobe combination. The same deforming rotor grid generated by SCORG<sup>®</sup> is used for performance calculation with both solvers. The performance is also measured on the test compressor in the test rig at City University London. Performance predictions obtained from CFD models are compared with measurement results. The compared performance indicators include pressure variation in the compressor chamber, mass flow rate, indicated power and the volumetric efficiency.

## 2. TEST CASE AND GRID GENERATION

The compressor used for this study is an oil-free twin screw compressor with a 3/5 lobe arrangement and 'N' rotor profile rotors. The operating speed on the male rotor varies from 6000 to 14000 rpm. The male rotor diameter is 127.45 mm; the female rotor diameter is 120.02 mm while the centre distance between the two rotors is 93.00 mm. The length to diameter ratio of the rotors is 1.6 and the male rotor has a wrap angle 285.0 deg. The nominal interlobe, radial and end leakage gaps are 160 micro meters each. The discharge port is designed for the built-in volume index of 1.8. Figure 2a shows the compressor mounted on the test rig.

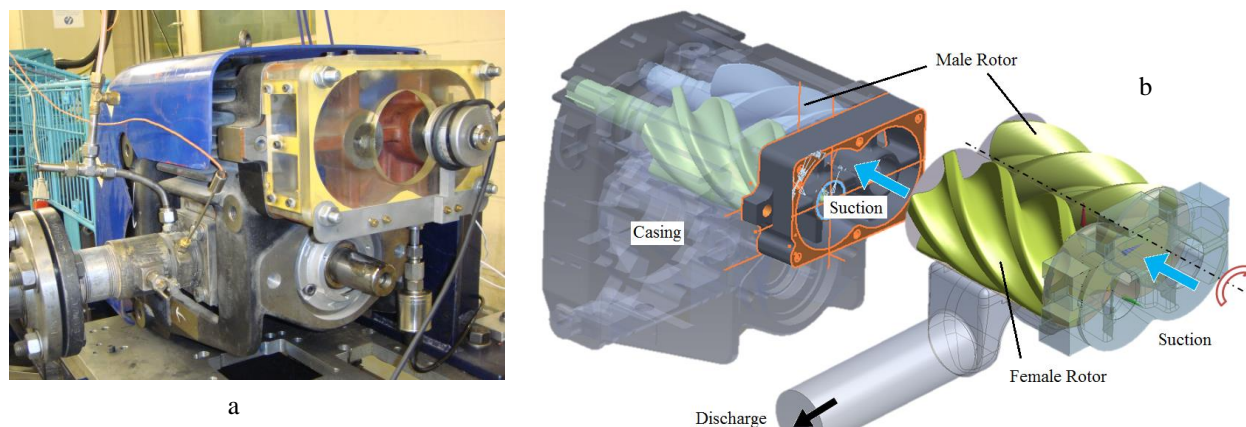


**Figure 2.** 3/5 N Rotor Screw Compressor – a) The Machine and b) Extracted Flow Model

The fluid domain is extracted from the CAD model and consists of three main parts: the suction, rotors and the discharge. Figure 2b shows the 3D CAD model of the compressor and the extracted fluid volumes. The suction and discharge ports are extended by circular pipes connected to the domains by explicitly connected interfaces. The grids of the rotor domains deform with the rotation of rotors. The proprietary, commercially available grid generator SCORG<sup>®</sup> was used to generate a set of grid files that are supplied to the solver as the simulation progresses. For details on the grid generation procedure refer to (*Kovacevic et al.*, 2007). During operation, the rotors are subject to thermal deformation which in turn changes the clearance. CFD models used in this research do not take into consideration changes in clearances. Therefore, it is estimated that the clearances will reduce with the increase in temperature and the grids for CFD are generated using reduced uniform clearances of 60 micro meters in the interlobe and radial gaps. The end clearances are not included in the CFD model. Figure 3a shows the structured

numerical grid on the rotor surfaces and Figure 3b shows the grid in the cross section of the rotor domain. The working fluid is air. A molar mass of 28.96 kg/kmol, Specific Heat Capacity  $1.0044e^{03}$  J/kg K, Dynamic Viscosity  $1.831e^{-05}$  kg/m s and Thermal Conductivity  $2.61e^{-02}$  W/m K were specified in both solvers. A uniform pressure of 1.0bar was specified at the suction while two cases with discharge pressures of 2.0bar and 3.0bar were analysed for a variety of speeds from 6000rpm to 14000rpm.

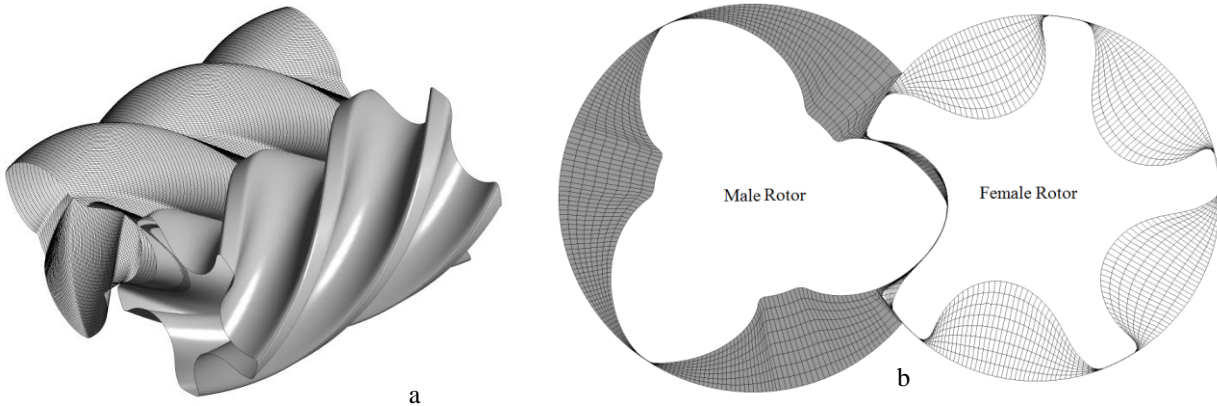


**Figure 3.** Grids in the Rotor domain – a) On the rotor surface and b) In the rotor cross section

### 3. PRESSURE BASED COUPLED SOLVER

The pressure based coupled solver (ANSYS CFX) will be referred to as Solver-1 and the segregated solver used in PumpLinx will be referred to as Solver-2. Solver-1 uses an Element-based finite volume method. Figure 4a presents a flow chart with an overview of the solution process used by a generic coupled solver whereas Figure 4b is a 2D illustration of the Element-based construction of the control volume.

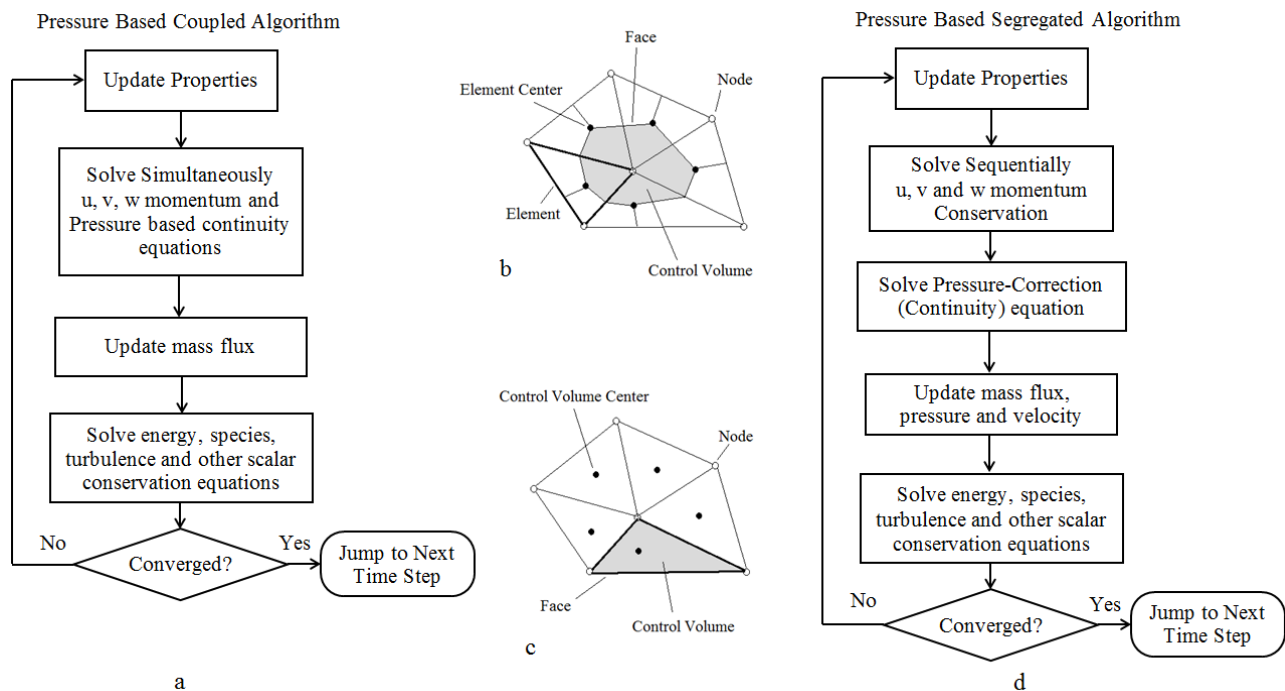


**Figure 4.** Overview of the Pressure based solver – a) Coupled Approach, b) Element-based control volume, c) Cell centred control volume and d) Segregated Approach

In the Element-based method of Solver-1, the spatial domain is firstly discretized into a mesh by using an external grid generator like SCORG©. This mesh is then used to construct virtual control volumes within the solver. All solution variables and fluid properties are stored at the nodes. A coupled system of equations comprising the momentum equations and the pressure-based continuity equation is solved in one step. The remaining equations, such as energy and turbulence, are solved in a decoupled fashion. The rate of convergence is expected to improve with this approach but the memory requirement increases 1.5–2 times compared to a segregated solver since the momentum and pressure-based continuity equations needs to be stored in the memory at the same time. Table 1 summarizes the important selection of Solver-1 parameters for a typical screw compressor analysis.

**Table 1.** Solver-1 Modelling Parameters (Used by ANSYS CFX)

Criteria	Selection	Remark	
<b>Mesh in Rotor</b>	Hexahedral + Pyramid	Generated by Customized Grid Generator	
<b>Mesh Deformation</b>	User Defined	Via Junction Box routines	Conservative
<b>Mesh in Ports</b>	Tetrahedral with Boundary layer refinements	Generated by Solver-1 pre-processor	Represented in Figure 5
<b>Turbulence Model</b>	SST – k Omega	Flow regime is Turbulent	
<b>Inlet Boundary Condition</b>	Opening	Specified Total Pressure and Temperature	Allows for flow to go in and out of the domain
<b>Outlet Boundary Condition</b>	Opening	Specified Total Pressure and Temperature	Allows for flow to go in and out of the domain
<b>Control Volume Gradients</b>	Gauss Divergence Theorem	Shape functions used to interpolate $\phi$	
<b>Advection Scheme</b>	Upwind	High Resolution	
<b>Pressure-Velocity Coupling</b>	Co-located layout	Rhie and Chow 4 <sup>th</sup> Order	
<b>Turbulence Scheme</b>	First Order Upwind		
<b>Transient Scheme</b>	Second Order	Backward Euler	Fully Implicit
<b>Transient Inner Loop Coefficients</b>	Up to 20 iterations per time step		
<b>Convergence Criteria</b>	1e-03	r.m.s residual level	
<b>Relaxation Parameters</b>	Solver relaxation fluids	0.1 or lower	For Stability



**Figure 5.** Solver-1 Tetrahedral Mesh

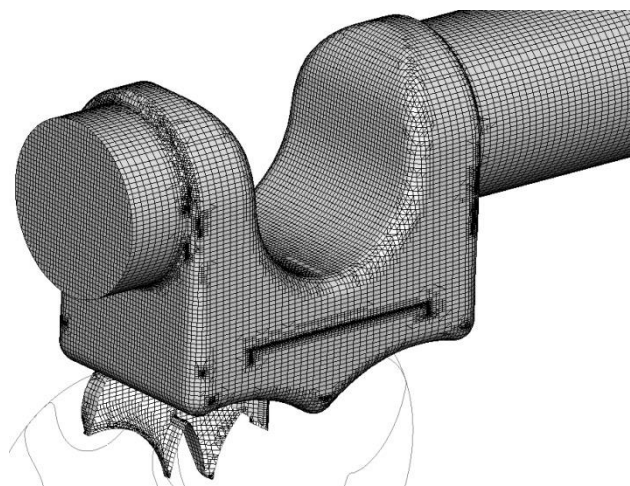


**Figure 6.** Solver-2 Body-fitted binary tree Mesh

#### 4. PRESSURE BASED SEGREGATED SOLVER

The pressure based segregated Solver-2 uses a cell-centred finite volume approach. Figure 4c is a 2D illustration of the cell centre based construction of the control volume. The cell-centre approach directly uses the mesh generated by the external grid generator to form control volumes. Figure 4d presents a flow chart with an overview of the solution process used by a generic segregated solver. The governing equations are solved separately for each variable. Firstly, the momentum equations are solved using the updated values of pressure and face mass fluxes. This is followed by the pressure correction equation. Face mass fluxes, pressure, and the velocity field are then corrected using the pressure correction obtained from a pressure-velocity coupling solution. The solution is then obtained iteratively until the convergence criteria are met. An important step in the segregated approach is the pressure-velocity coupling algorithm. Many algorithms, Simple, SimpleC, PISO, SimpleS (Simerics proprietary) etc., have been developed over years to improve the robustness of this approach. The segregated algorithm is memory-efficient, since the discretized equations need only to be stored in the memory one at a time. Table 2 summarizes the important Solver-2 parameters and their selections for a typical screw compressor analysis.

**Table 2.** Solver-2 modelling parameters (Used by PumpLinx)

Criteria	Selection	Remark	
<b>Mesh in Rotor</b>	Hexahedral + Pyramid	Generated by Customized Grid Generator	
<b>Mesh Deformation</b>	Screw Compressor Template		Conservative
<b>Mesh in Ports</b>	Body-fitted binary tree	Generated by Solver-2 pre-processor	Represented in Figure 6
<b>Turbulence Model</b>	k-epsilon RNG	Flow regime is Turbulent	
<b>Inlet Boundary Condition</b>	Pressure Inlet or Total Pressure	Specified Static/Total Pressure and Static/Total Temperature	
<b>Outlet Boundary Condition</b>	Pressure Outlet	Specified Static Pressure and Temperature	
<b>Advection Scheme</b>	Upwind	First/Second Order	
<b>Pressure-Velocity Coupling</b>	Co-located Layout	SIMPLE S	Simerics Proprietary
<b>Turbulence Scheme</b>	First Order Upwind		
<b>Transient Scheme</b>	First Order	Backward Euler	Fully Implicit
<b>Transient Inner Loop Coefficients</b>	Up to 25 iterations per time step		
<b>Convergence Criteria</b>	1e-02	r.m.s residual level	
<b>Relaxation Parameters</b>	Pressure	0.5	For Stability

#### 5. EXPERIMENTAL RESULTS

Experimental investigation of the compressor performance was carried out in the air compressor test rig at City University London. Figure 7 presents the layout of the measurement setup with the main components and measurement points. The compressor is driven by a variable speed 75kW motor and has an internal synchronizing gear box with the gear ratio 7.197:1. The speed of the motor is adjusted using a variable frequency drive. The torque meter is installed on the motor shaft while the digital encoder for the speed measurement is mounted on the male rotor shaft. Figure 2 shows the compressor in the test rig. The pressure and temperature of the gas are measured at the inlet, the discharge and upstream of the orifice plate. In addition, three pressure transducers are used for recording the interlobe pressures and are located in the working chamber through the compressor casing on the male rotor side. The flow through the compressor is measured by use of an orifice plate installed in the discharge line of the system. The discharge line contains a control valve for regulation of the discharge pressure. The data acquisition is carried out using CompactRIO from National Instruments and Labview. The measurements were taken for discharge pressures up to 2.5bar and speeds from 6000 to 8000rpm.

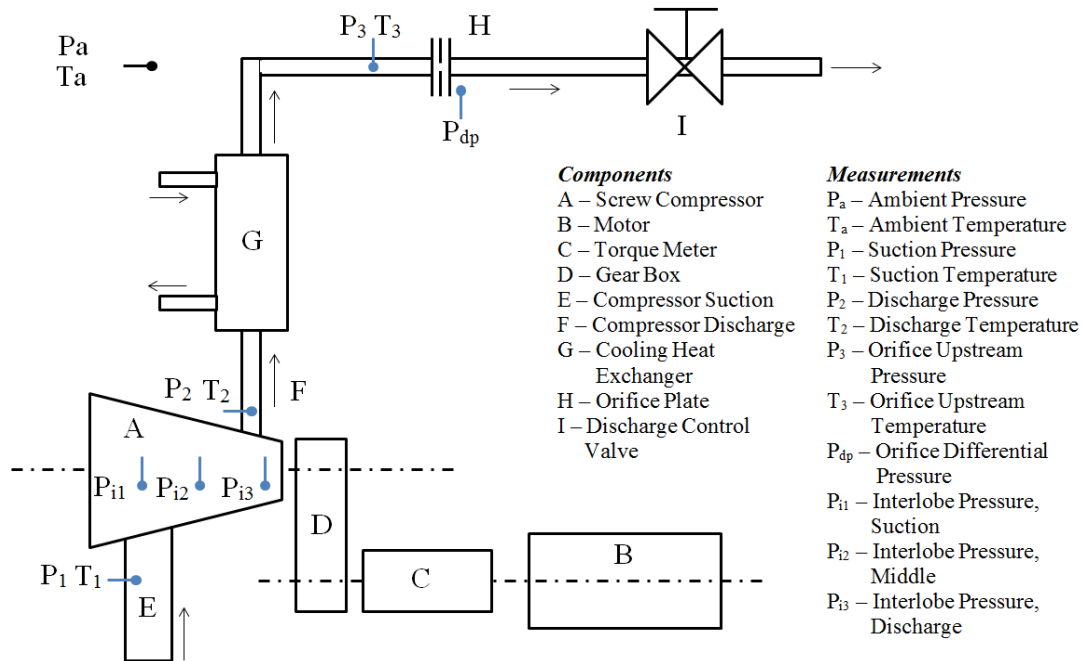


Figure 7. Experimental setup for screw compressor performance measurement

## 6. COMPARISON OF RESULTS AND DISCUSSION

The results obtained from CFD modelling are compared with the experimental results in the sections that follow.

### 6.1 Pressure-Angle Diagram

Figure 8 shows the variation of the chamber pressure with the angle of rotation of the male rotor at two speeds, 6000 and 8000rpm. The results from CFD calculation are compared with experimental data.

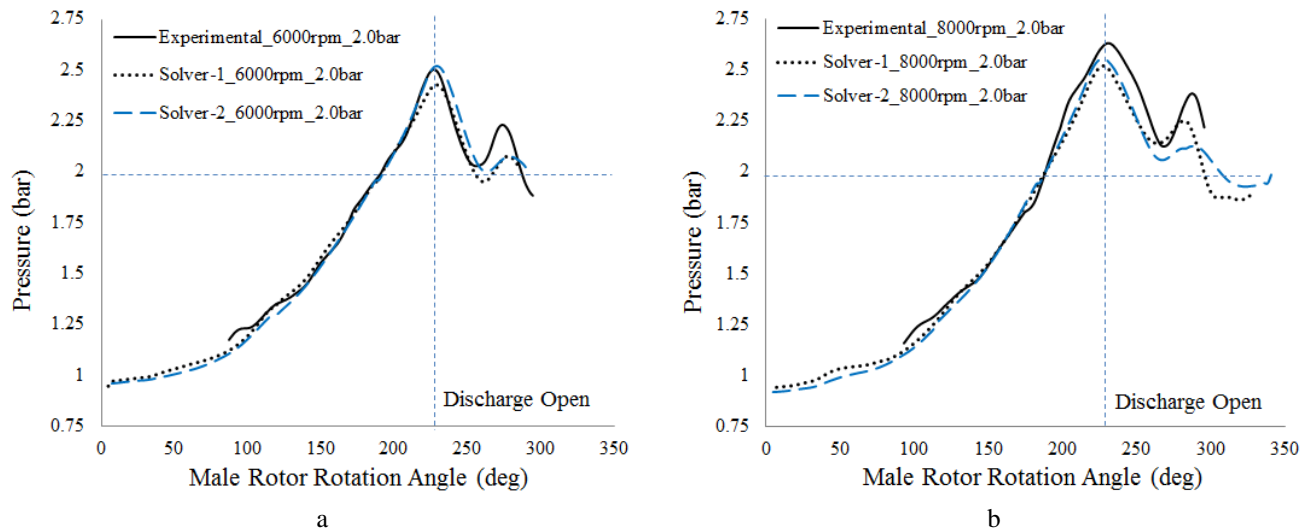
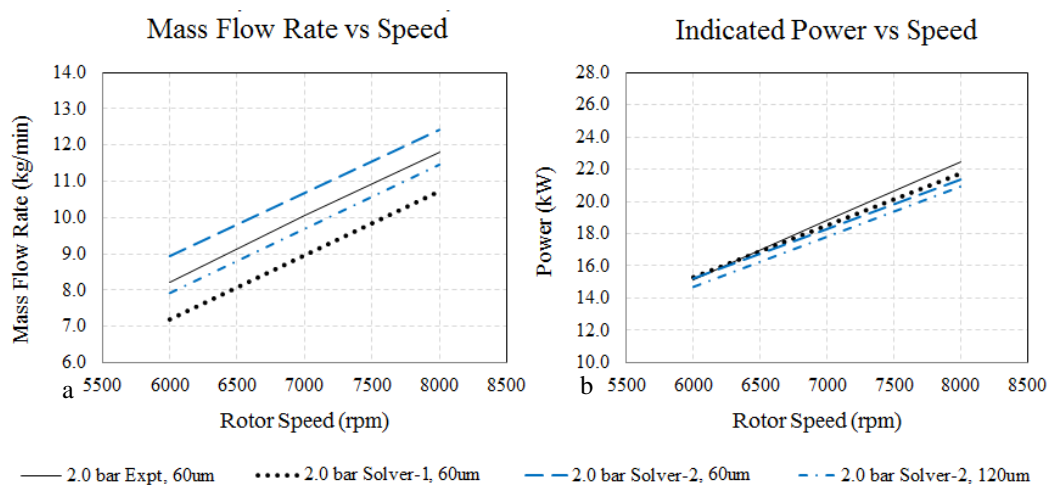


Figure 8. Pressure-Angle diagram comparison at 2.0bar discharge pressure for a) 6000 rpm, b) 8000 rpm

The internal pressure calculated by both solvers is agreeing well with the measured pressure curve at both speeds. Some differences between predictions and measurements are noticed near the peak pressure at the moment of opening of the discharge port. Solver 2 shows slightly better agreement with measured data.

## 6.2 Mass Flow rate

Figure 9a shows the comparison of the flow predictions from the CFD calculations with experimental data and Figure 10a shows the comparison between the two solvers over the full range of speeds and pressures. Solver-2 is predicting higher mass flow rate as compared to Solver-1 and is closer to the experimental results. The predicted mass flow rate depends on the assumption of clearances. A smaller clearance would result in higher flow rates and vice versa. The assumed clearance gap was 60 micrometres. In order to determine the sensitivity of the results to the clearances, another calculation was performed with Solver-2 with a clearance of 120 micrometres. As shown in Figure 9a, this resulted in a flow rate lower than the measured. This indicates that the average physical clearance is between 60 and 120 micrometres, probably around 100 micrometres in this case. It is known that the clearances in the rotor domain are varying non-uniformly with operating conditions and the assumption of average clearances may introduce inaccuracy. Therefore, further studies are needed in order to confirm if the lower than measured flow predicted by Solver-1 is due to the coupled solution approach or some other factors.



**Figure 9.** Comparison of Experimental and CFD Predictions of a) Mass Flow Rate and b) Indicated Power

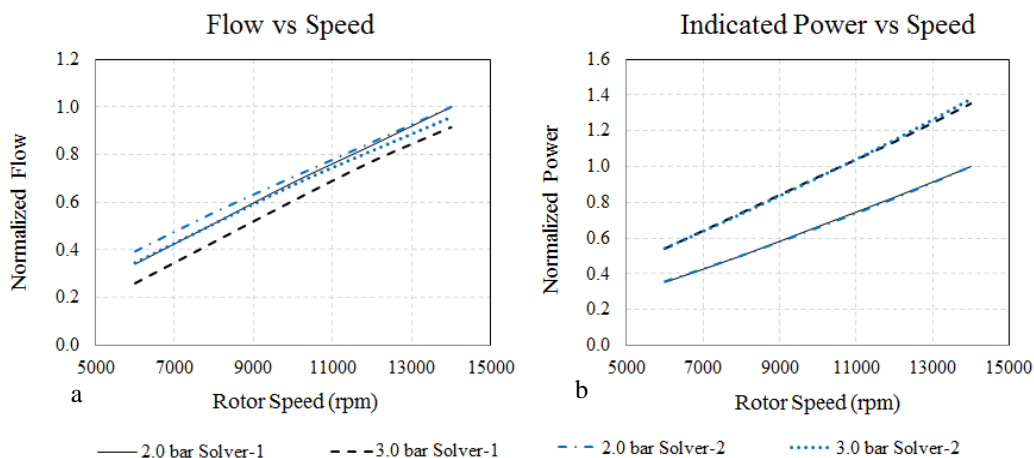


**Figure 10.** Comparison of CFD Predictions with 60um clearance over full range of a) Flow and b) Indicated Power

## 6.3 Indicated Power

In the experiment, the power was measured on the motor shaft and a constant mechanical efficiency of 95% was assumed for the integral gearbox at all speeds. Figure 9b shows the comparison of the indicated power prediction from CFD calculations with experimental data and Figure 10b shows the comparison between the two solvers over the full range. Both solvers are predicting similar indicated power which is very close to the experimental results. The assumption of the constant mechanical efficiency of the gearbox is not the most accurate since the efficiency of the gearbox changes with speed. Despite this, the agreement in power prediction is good.

#### 6.4 Specific Power and Volumetric Efficiency

Specific power is the ratio of the indicated power and flow through the compressor. A lower specific power indicates a better machine. Figure 11a compares the specific power prediction from the CFD calculations with the experimental data and Figure 12a shows the comparison between the two solvers over the full range. Results obtained from Solver-2 are closer to the experimental results and could be further improved by specifying clearances closer to the expected real values.

Figure 11b compares the volumetric efficiency prediction from the CFD calculations with the experimental data and Figure 12b shows the comparison between the solvers over the full range. Efficiencies obtained from Solver-2 are closer to the experimental results and could be further improved by specifying accurate clearances. As the compressor speed increases the volumetric efficiency increases. Both solvers predict the same trend.

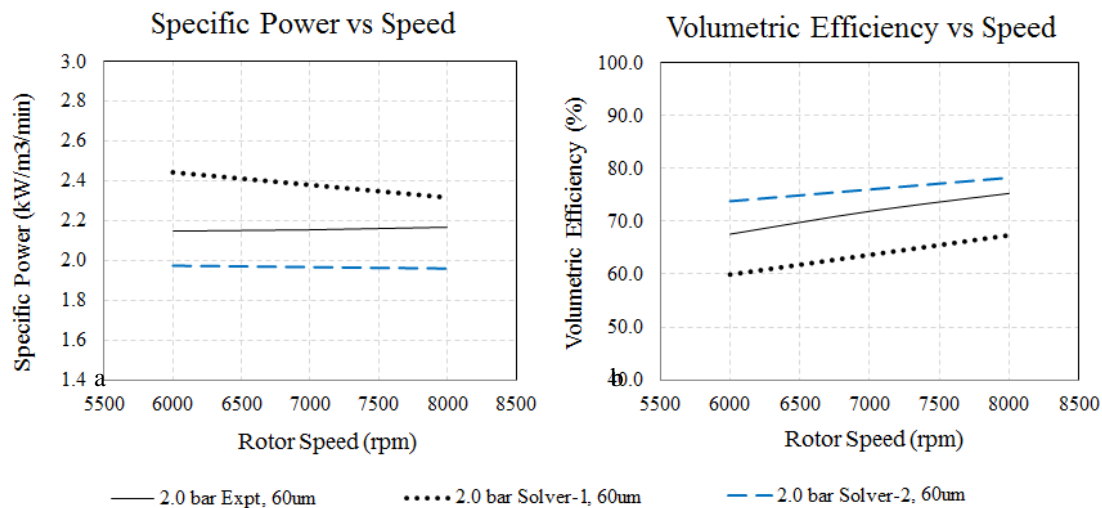


**Figure 11.** Comparison of Experimental and CFD Predictions of a) Specific Power and b) Volumetric Efficiency

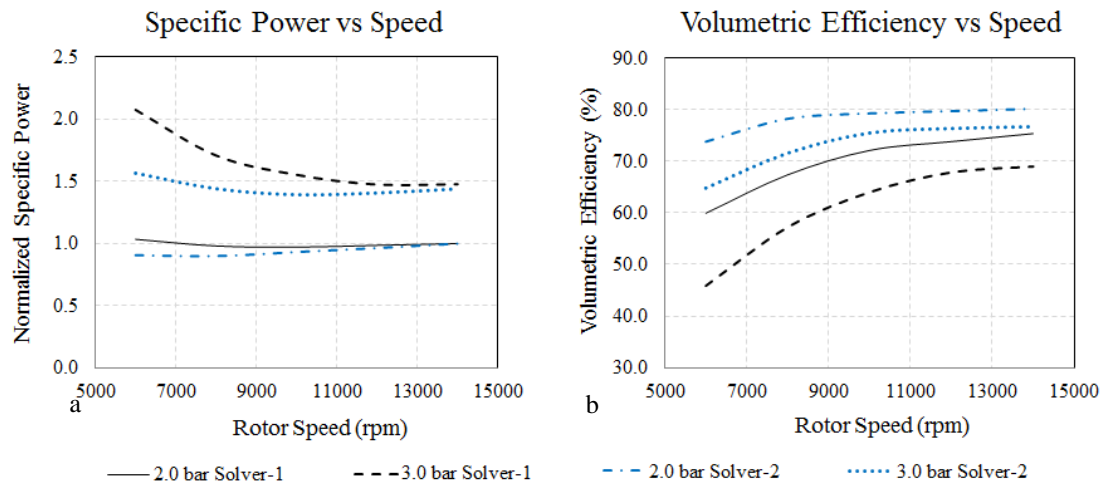


**Figure 12.** Comparison of CFD Predictions with 60um clearance of a) Specific Power and b) Volumetric Efficiency

The study revealed differences in performance predictions between the two CFD solvers and also deviations compared with the experimental results. The time required for the segregated cell-centre Solver-2 to reach a cyclic solution is about one third of the coupled Solver-1; it is less memory intensive and resulted in flow predictions closer to the experimental values.

## 7. CONCLUSIONS

Flow in a twin screw compressor was modelled using two different CFD solvers which have different approaches to discretisation and solution of the governing equations. Performance predictions were obtained over a range of speed and pressure ratios of the oil free air compressor. These performance parameters were also measured on a test rig. The following conclusions can be derived from comparison of the results in this study:

- Differences exist between the two solvers in the prediction of flow rates through the compressor. Comparison with experimental data suggests that Solver-2 is giving more accurate estimation of flow rates for the expected clearances.
- In the future, it will be required to carry out further studies in order to establish the reason for under prediction of the flow by the coupled solver used in Solver-1.
- Both solvers are predicting indicated power close to the experimental data.
- Operational clearances are changing due to the change in temperature for different operating conditions. In order to obtain accurate predictions, this change should be accounted for in the CFD models in future. This may require employment of fluid solid interaction modelling.

This study provides a good basis for further consideration of the application of variable leakage gaps based on empirical or analytical correlations and also in improvements of differencing schemes and other settings required for specific CFD solvers. Availability of extended data from the experimental measurements will be beneficial for comparison over a wider range of operating conditions and will help improve the CFD models.

## REFERENCES

- ANSYS 13.0, 2011, User help.
- Hanjalic K., Stosic N., 1997, Development and Optimization of Screw machines with a simulation Model – Part II: Thermodynamic Performance Simulation and Design Optimization. Transactions of the ASME 664 / Vol. 119
- Hauser J. and Beinert M., 2013, CFD analysis of pressure pulsation in screw compressors - combine theory with practice. 8th Int conf on compressors and their systems, p. 625.
- Jiang Y., Furmanczyk M., Lowry S., Zhang D., and Perng Chin-Yuan, 2007, A Three-Dimensional Design tool for Crescent Oil Pumps. SAE p. 2008-01-0003.
- Kauder K., Rau B., 1994, Auslegungsverfahren für Schraubenkompressoren. (Design Procedure for screw compressors), VDI Berichte 1135, S. 31-44, Düsseldorf: VDI-Verlag.
- Kovacevic A., 2002, Three-Dimensional Numerical Analysis for Flow Prediction in Positive Displacement Screw Machines, Ph.D. Thesis, School of Engineering and Mathematical Sciences, City University London, UK.
- Kovacevic A., Stosic N. and Smith I. K., 2007, Screw compressors - Three dimensional computational fluid dynamics and solid fluid interaction, ISBN 3-540-36302-5, Springer-Verlag Berlin Heidelberg New York.
- Kovacevic A., Stosic N., Smith I. K., Mujic E., and Guerrato D., 2009, Extending the role of computational fluid dynamics in screw machines, 6<sup>th</sup> Int conf on compressors and their systems, p. 41.
- Kethidi M., Kovacevic A., Stosic N. and Smith I. K., 2011, Evaluation of various turbulence models in predicting screw compressor flow processes by CFD. 7<sup>th</sup> Int conf on compressors and their systems, p. 347.
- Kovacevic A. and Rane S., 2013, 3D CFD analysis of a twin screw expander, 8th International conference on compressors and their systems, London, p. 417.
- Pascu M., Kovacevic A., and Udo N., 2012, Performance optimization of Screw Compressors based on numerical investigation of the flow behaviour in the discharge chamber. Int Compressor Conf at Purdue, Purdue, p. 1145.
- PumpLinx 3.2.2, 2014, User help.
- Rane S., Kovacevic A., Stosic N. and Kethidi M., 2013, CFD grid generation and analysis of screw compressor with variable geometry rotors, 8<sup>th</sup> Int conf on compressors and their systems, p. 601.
- Sauls J. and Branch S., 2013, Use of CFD to develop improved one-dimensional thermodynamic analysis of refrigerant screw compressors. 8th Int conf on compressors and their systems, p. 591.
- Stosic N., 1998, On Gearing of Helical Screw Compressor Rotors, Proceeding of IMechE, J. Mech. Eng. Science, Vol.212, and pp. 587.
- Voorde John Vande and Vierendeels Jan, 2005, A grid manipulation algorithm for ALE calculations in screw compressors. 17th AIAA Computational Fluid Dynamics Conference, Canada, AIAA 2005-4701.
- Wang D., Ding H., Jiang Y. and Xian X., 2012, Numerical modeling of vane oil pump with variable displacement. SAE Paper 2012-01-0637.